The role of the endoplasmic reticulum stress response following cerebral ischemia

Gina Hadley[1], Ain A Neuhaus[1], Yvonne Couch[1], Daniel J. Beard[1], Bryan A. Adriaanse[3], Kostas Vekrellis[2], Gabriele C DeLuca[3], Michalis Papadakis[1], Brad A Sutherland[1,4,*], Alastair M. Buchan[1,5,6,*]

[1] Acute Stroke Programme, Radcliffe Department of Medicine, University of Oxford, Oxford, United Kingdom

[2] Department of Neuroscience, Center for Basic Research, Biomedical Research Foundation of the Academy of Athens, Athens, Greece

[3] Nuffield Department of Clinical Neurosciences, University of Oxford, Oxford, UK.

[4] School of Medicine, Faculty of Health, University of Tasmania, Hobart, Australia

[5] Medical Sciences Division, University of Oxford, Oxford, UK

[6] Acute Vascular Imaging Centre, University of Oxford, Oxford University Hospitals, Oxford, UK

[*] Joint senior authors

Corresponding author:

Professor Alastair Buchan

Medical Sciences Division

University of Oxford

John Radcliffe Hospital

Headington

Oxford

OX3 9DU

tel: +44 (0)1865 220346

email: alastair.buchan@medsci.ox.ac.uk

Keywords: autophagy, endogenous neuroprotection, ER stress, global ischemia, hamartin, mTOR, OGD, TSC1

List of tables and figures:

Abstract

Background: Cornu Ammonis 3 (CA3) hippocampal neurons are resistant to global ischemia whereas Cornu Ammonis 1 (CA1) neurons are vulnerable. Hamartin expression in CA3 neurons mediates this endogenous resistance via productive autophagy. Neurons lacking hamartin demonstrate exacerbated endoplasmic reticulum (ER) stress and increased cell death. We investigated ER stress responses in CA1 and CA3 regions following global cerebral ischemia, and whether pharmacological modulation of ER stress or autophagy altered neuronal viability.

Methods: In vivo: male Wistar rats underwent sham or 10 min of transient global cerebral ischemia. CA1 and CA3 areas were microdissected and ER stress protein expression quantified at 3 h and 12 h of reperfusion. *In vitro*: primary neuronal cultures (E18 Wistar rat embryos) were exposed to 2 h of oxygen and glucose deprivation (OGD) or normoxia in the presence of an ER stress inducer (thapsigargin or tunicamycin), an ER stress inhibitor (salubrinal or 4-phenylbutyric acid (4-PBA)), an autophagy inducer ([4'-(N-diethylamino) butyl]-2-chlorophenoxazine (10-NCP)) or autophagy inhibitor (3-methyladenine (3-MA)).

Results: In vivo, decreased ER stress protein expression (phospho-eIF2α and ATF4) was observed at 3 h of reperfusion in CA3 neurons following ischemia, and increased in CA1 neurons at 12 h of reperfusion. *In vitro*, ER stress inducers and high doses of the ER stress inhibitors also increased cell death. Both induction and inhibition of autophagy also increased cell death.

Conclusion: Endoplasmic reticulum stress is associated with neuronal cell death following ischemia. Neither reduction of ER stress nor induction of autophagy demonstrated neuroprotection *in vitro* highlighting their complex role in neuronal biology following ischemia.

Introduction

Experimental therapies for stroke have thus far focused on suppressing the ischemic cascade, the biochemical activation of numerous intracellular pathways leading to neuronal injury. One alternative approach is to amplify neuroprotective mechanisms that are endogenously active in cells. In the hippocampus, CA1 neurons are susceptible to ischemic death while CA3 neurons appear resistant (1). We have previously shown that endogenous CA3 neuroprotection is mediated through hamartin, an upstream inhibitor of mammalian target of rapamycin (mTOR) via induction of productive autophagy (2). In addition to differences in autophagy, the tuberous sclerosis complex (TSC, in which hamartin (TSC1) and tuberin (TSC2) are key components) has been implicated in neuronal stress responses. Neurons lacking TSC have increased vulnerability to endoplasmic reticulum (ER) stress-induced cell death (3). With loss of TSC function, there is uncontrolled mTOR hyperactivation, which results in an increase in protein synthesis and ROS production, and is detrimental to neurons.

Physiologically, the ER receives proteins targeted for secretion, as well as proteins that will be incorporated into the ER, the Golgi apparatus, the plasma membrane and lysosomes. Proteins destined for the cytosol, mitochondria and nucleus are synthesised on free ribosomes in the cytosol and released (as reviewed in (4)). Under conditions of cellular stress, where the build-up of proteins exceeds the capacity of the ER, an unfolded protein response (UPR) occurs (5). The UPR is a homeostatic mechanism by which cells regulate levels of misfolded proteins in the ER. It has three specialized stress sensors located at the ER membrane: inositol-requiring enzyme 1 (IRE1), activating transcription factor 6 (ATF6) and protein kinase RNA-like ER kinase (PERK) (6). The suppression of most protein translation occurs via the phosphorylation of eukaryotic translation initiation factor 2 subunit α (eIF2α) by PERK. Phospho-eIF2α globally inhibits translation except for the selective translation of the mRNA encoding the transcription factor ATF4 (CREB 2), which controls the expression of various genes involved in the stress response.

Differences in the ER stress response between CA1 and CA3 have been demonstrated previously. Phospho-eIF2α and phospho-PERK were increased in CA1 neurons compared to CA3 neurons in wild type rats exposed to global ischemia, which was attenuated in copper/zinc superoxide dismutase transgenic rats (7). This result links the production of ROS with modification of ER stress proteins and implicates ER stress in neuronal cell death. Moreover, the ER stress response was stronger in CA1 than CA3 neurons, which was associated with their differential survival following ischemia (8). However, our experiments are the first to pharmacologically manipulate pathways downstream of harmartin, in this context to further elucidate the protective mechanism of hamartin and establish whether directly altering ER stress or autophagy could provide neuroprotection.

Aims

Our aim was to elucidate the role of ER stress in the previously identified phenomenon of hamartin-mediated neuroprotection. Initially, the acute timecourse of ER stress protein expression in response to global ischemia was determined in both vulnerable (CA1) and resistant (CA3) hippocampal neurons. Furthermore, we assessed whether modulation of the ER stress response and autophagy *in vitro* could replicate neuroprotection induced by hamartin.

Materials and Methods

Animals

Adult male Wistar rats (150-200g) were obtained from Harlan, UK. Animals were housed in a standard light:dark cycle (12/12 h) and had access to food and water *ad libitum.* All procedures were conducted in accordance with the Animals (Scientific Procedures) Act, 1986 and were approved by the Home Office (UK) and Animal Care and Ethical Review committee (University of Oxford).

Experimental protocols

Figure 1 shows the experimental timeline for each of the presented experiments. For our first aim, we exposed rats to the global cerebral ischemia model for 10 min and then assessed hamartin expression and the ER stress response through immunoblotting at 3 h and/or 12 h of reperfusion (Figure 1A). For our second aim, we isolated neurons from the cortices of embryonic rats, exposed these neurons to oxygen and glucose deprivation (OGD) in the presence or absence of ER stress inducers or inhibitors, or autophagy inducers or inhibitors, and assessed neuronal viability using the lactate dehydrogenase assay (Figure 1B).

Global cerebral ischemia

Animals underwent transient global cerebral ischemia using the modified four vessel occlusion (4-VO) model as previously described (2). Briefly, rats were anesthetised with isoflurane (3% v/v induction, 1-1.5% v/v maintenance carried in 30% O_2 (v/v) and 70% N_2O (v/v)) and underwent pre-4-VO surgery. Pre-4-VO entailed exposure, dissection and loose ligation of both common carotid arteries, placement of a 2-0 braided silk suture through the neck to control collateral circulation, and cauterization of both vertebral arteries to restrict posterior circulation. Rats were allowed to recover for 24 h (with access to water only) before undergoing 4-VO. At 24 h, rats were then re-anesthetised, both common carotid arteries were occluded and the neck suture was tightened (4-VO). This diminished anterior and collateral circulation with posterior circulation already restricted. Global ischemia was confirmed by meeting a number of clinical criteria including pupil dilation, presence of a running response, absence of corneal and pain reflexes and loss of righting response. Ischemia was maintained for 10 min, after which the clips and sutures were released and the animals allowed to recover. All animals received buprenorphine analgesia

(0.1mg/kg subcutaneously) and topical local anaesthesia (lidocaine ointment) following surgery. Temperature, which can modify ischemic pathophysiology, was maintained during surgery with a homeothermic blanket and during recovery by a telemetry feedback system (TA-F40, Data Sciences International). Sham animals underwent pre-4-VO surgery as described above but did not receive common carotid artery and collateral occlusion.

Immunoblotting

Rats were killed immediately following the required period of reperfusion (3 and 12 h) by terminal anaesthesia and decapitation. Rat brains were dissected and the CA1 and CA3 subregions of the hippocampus were microdissected from 2mm coronal sections. Samples were snap frozen on dry ice and remained at -80°C until processing. Brain tissue was homogenized with a glass:glass homogenizer in homogenization buffer (50mM Tris HCl, 150mM NaCl, 1% Triton X-100, 1mM EDTA, 0.1% sodium dodecyl sulfate (SDS), pH 7.4) supplemented with 1mM PMSF, protease inhibitor cocktail (Roche Diagnostics) and a phosphatase inhibitor cocktail (PhosSTOP, Roche Diagnostics). Homogenates were incubated for 30 min using a rotary platform at 4°C and then spun at 16,000 x g for 30 min at 4°C. The supernatant was transferred to an Eppendorf tube at 4°C. The pellet was resuspended in 200µl of homogenisation buffer and centrifuged at 16,000 x g for 30 min at 4°C. The supernatant was pooled with the previous supernatant and stored at -80°C. Protein content was ascertained using a bicinchoninic acid assay (BCA).

Whole cell homogenates were defrosted and proteins were precipitated using the methanol/chloroform technique (2, 9). The protein pellet was resuspended in Laemmli sample buffer (Biorad) with 10mM dithiothreitol and denatured at 95°C for 5 min. 25µg protein was loaded onto Criterion Tris-HCl Precast 7.5% or 15% gels (Biorad), in a chamber filled with running buffer (final concentration 25mM tris base, 200mM glycine and 0.1% (w/v) SDS in distilled water). One lane was used to determine molecular weight. The gel underwent electrophoresis (110V for 2 h) before cold transferring to a polyvinylidene difluoride (PVDF) membrane (100V for 30 min in transfer buffer (25mM tris base, 200mM glycine and 10% methanol in distilled water)). Quantification of loading was carried out using SYPRO® reagent (Life Technologies) using manufacturer's instructions. Six-band analyses were conducted to quantify protein loading using the UVP Biospectrum AC imaging system (see Supplementary Fig.1). After SYPRO staining, the membrane was washed and blocked with 5% w/v milk powder in PBS (Sigma) for 1 h at room temperature. The membrane was incubated with the appropriate primary antibody in 5% milk powder in PBS and left overnight at 4°C. Primary antibodies used in this study were: 1:1000 rabbit anti-hamartin (ab25882, Abcam); 1:600 rabbit anti-ATF4/CREB-2 (C-20) (sc-200, Santa Cruz); and 1:1000 rabbit anti-phospho-eIF2α (Ser^{51}) (9721, Cell Signalling). After washing, membranes were incubated in goat anti-rabbit IgG horseradish peroxidase (HRP) secondary antibody (diluted in 5% w/v milk powder in PBS) for 1 h at room temperature. Chromogen detection was determined through enhanced chemiluminescence (GE Healthcare) and imaged using the Biospectrum AC imaging system and VisionWorks software (UVP). The bands were quantified by densitrometry and corrected for loading using the quantified SYPRO® data. Membranes probed for more than one antibody (Supplementary Figure 1, antibody to ATF4 probed and then antibody to phospho-eIF2α) were stripped by washing for 5 min PBS-T, 10 minutes Blot Restore Solution A (Millipore), 15 minutes Blot Restore Solution B (Millipore), 5 min PBS-T and further blocking with 2 x 5 min 5% w/v milk powder.

Primary cortical neuron cultures

Cortical neuronal cultures were prepared from E18 Wistar rat embryos as previously described (2, 10). Briefly, embryonic cortices were microdissected and digested (0.05% trypsin and 100µg/ml DNAse in neurobasal medium (Gibco) with trypsin subsequently inhibited with 10% fetal bovine serum), the cell pellet was isolated by centrifugation (400 x g for 5 min) and resuspended in complete neurobasal medium (2% B27 serum-free supplement (Gibco), 2mM L-glutamine and 1% penicillin/streptomycin in neurobasal medium). Cells were plated on poly-D-lysine coated 12-well plates at 5 x 10^5 cells per well (1.25 x 10^5 cells/cm^2) and incubated in a standard humidified incubator (37°C, 5% CO_2).

Oxygen and glucose deprivation

Oxygen and glucose deprivation (OGD) was used as an *in vitro* surrogate for ischemic stroke. At days in vitro (DIV) 7-8, mature neurons were exposed to deoxygenated neurobasal medium without D-glucose and sodium pyruvate (Neurobasal-A, Invitrogen) in a 0% O_2 environment using a hypoxic chamber (Coy) for 2 h. Normoxic controls were exposed to oxygenated Neurobasal-A medium supplemented with 25mM D-glucose and remained in a standard incubator for 2 h. Following OGD or normoxia, neurons underwent recovery with fresh complete neurobasal medium for 24 h under standard incubation conditions (37°C, 5% CO_2).

Cell death assay

Cell death in primary neuronal cultures was assessed quantitatively using the lactate dehydrogenase (LDH) release assay (Cytotox96 assay, Promega). Media were collected at the end of 2 h and 24 h recovery periods, and cells were lysed with 1% Triton X-100 in complete neurobasal medium to determine total LDH released. Measurements were carried out in technical triplicate for at least $n = 3$ biological replicates. Results were expressed as a percentage of the amount of LDH released in the cell culture medium to the total LDH content in the same cultures.

Pharmacology

To determine the influence of ER stress on neuronal viability following OGD, pharmacological agents that can modulate ER stress were investigated. Thapsigargin (Sigma) (0.01-10μM) and tunicamycin (Sigma) (0.01-1μM) were used to induce ER stress, while salubrinal (Santa Cruz Biotechnology) (25-500μM) and 4-Phenylbutyric acid (4-PBA) (Sigma) (10μM-10mM) were used to inhibit ER stress. To investigate modulation of autophagy, 10-NCP (BioVision) (0.1-10μM) was used to induce autophagy and 3MA (Sigma) (0.1-10μM) was used to inhibit autophagy. All drugs were administered during the 2 h OGD/normoxia period. The vehicle control was either media alone or 2% DMSO in OGD/normoxia media.

Statistical analyses

Statistical analysis was carried out with GraphPad Prism 5 using a two-tailed Student's t-test if two groups were compared. For comparisons of more than two groups with two independent variables, a two-way ANOVA with a Dunnett's post hoc testing comparing all groups to the control group (vehicle) was used. Differences were considered significant for $p < 0.05$. Data are presented as mean ± SEM.

Results

Hamartin expression is reduced following global ischemia

Given our previous findings showing hamartin mediated neuroprotection (2) and the potential links to ER stress modulation, we initially investigated the expression of hamartin *in vivo* following ischemia. At 3 h following 10 min of global cerebral ischemia, hamartin expression was significantly decreased in the vulnerable CA1 of ischemic animals compared to CA1 of sham animals (*p*=0.003) (Fig 2).

ER stress reduction in tolerant CA3 at 3 h while ER stress induction in vulnerable CA1 at 12 h was seen following global ischemia

To examine the role of ER stress in the endogenous resistance of CA3 neurons to global ischemia, CA1 and CA3 areas of the hippocampus were dissected following 10 min of global cerebral ischemia and reperfusion times of 3 h or 12 h. ATF4 expression was used to assess ER stress levels. At 3 h, there was no significant difference in ATF4 expression between CA1 of sham animals and CA1 of ischemic animals (*p*=0.1106) (Fig. 3A). However, in CA3 neurons there was significantly lower ATF4 following ischemia compared to sham (*p*=0.0396) (Fig. 3B)). At 12 h following transient global forebrain ischemia there was significantly higher ATF4 (*p*=0.0142) in ischemic CA1 compared to sham (Fig. 3C) whereas there was no significant difference in ATF4 expression (*p*=0.6158) between CA3 of sham and ischemic animals (Fig. 3D).

To corroborate these findings, phospho-eIF2α protein expression levels were also used to assess ER stress levels at 3 and 12 h following transient global forebrain ischemia. As with ATF4, there were significantly lower levels of phospho-eIF2α protein expression in CA3 at 3 h following ischemia compared to sham (*p*=0.0206). (Fig. 4A) and phospho-eIF2α expression was significantly higher (*p*=0.015) in CA1 at 12 h following ischemia compared to sham (Fig. 4B).

Pharmacological induction of ER stress is neurotoxic in *an in vitro* model of ischemia

We sought to determine whether induction of ER stress caused an increase in neuronal cell death. We employed an ER stress inducer, thapsigargin, which inhibits Ca^{2+}-ATPase on the sarcoendoplasmic reticulum (11). Cortical neurons underwent 2 h of OGD or normoxia and were treated with thapsigargin during this time. Two-way ANOVA analysis revealed a significant effect of OGD (*p*<0.0001) and treatment (*p*<0.0001) during the 2 h. During 2 h of normoxia, thapsigargin had no effect on neuronal death, whereas during 2 h of OGD, 10µM thapsigargin significantly increased cell death when compared to control (p<0.0001, Fig. 5A). Similar effects of OGD (*p*<0.0001) and treatment (*p*<0.0001) were observed after 24 h of recovery from normoxia or OGD (Fig. 5B). Under both normoxic (*p*<0.0001) and OGD conditions (*p*<0.0001), 10µM thapsigargin caused significantly more cell death compared to DMSO controls (Fig. 5B). There was also a significant interaction between OGD and treatment at both time points (*p*<0.0001).

These results were corroborated by an additional ER stress inducer, tunicamycin, which inhibits N-glycosylation of proteins (12). At 2 h of OGD or normoxia with tunicamycin treatment (Fig. 5C), there was a significant effect of OGD (*p*=0.0042) and treatment (*p*=0.0044), with 1µM tunicamycin significantly increasing neuronal death following OGD (*p*=0.0100). After 24 h of recovery from OGD or normoxia (Fig. 5D), there was a significant effect of OGD (*p*=0.0360) and treatment (*p*=0.0233) (two-way ANOVA) with no significant differences between groups. There was no interaction between OGD and treatment at either timepoint.

Pharmacological inhibition of ER stress is neurotoxic in an *in vitro* model of ischemia

Given that ER stress induction showed neurotoxic effects, we then tested whether an ER stress inhibitor would attenuate cell death caused by OGD. We used salubrinal, a small molecule that prevents formation of GADD34/PP1 complex therefore reducing the dephosphorylation of phospho-eIF2α and inhibiting ER stress (13). At 2 h of OGD or normoxia with salubrinal treatment (Fig. 6A), there was a significant effect of OGD (*p*<0.0001) but no effect of treatment (*p*=0.3964) on cell death. After 24 h of recovery from OGD or normoxia with salburinal treatment (Fig. 6B), there was a significant effect of OGD (*p*=0.0024) and treatment (*p*<0.0001). Here, higher concentrations of salubrinal led to greater levels of cell death under both normoxia and OGD conditions (normoxia: 200µM *p*=0.0225, 500µM *p*=0.0223; OGD: 200µM *p*=0.0032, 500µM *p*=0.0001). There was no interaction between OGD and treatment at either timepoint. All groups were compared to DMSO control.

The trend of increased neuronal death at high concentrations demonstrated by these results was replicated using the chemical chaperone, 4-PBA known to help correct the folding of proteins and which has been shown to lessen the effects of ER stress in both animal models (14) and cell lines (15). At 2 h of OGD or normoxia with 4-PBA treatment (Fig. 6C), there was a significant effect of OGD (*p*<0.0001) treatment approached, but did not have a significant effect, on cell death (*p*=0.0541) on cell death. There was a significant interaction between OGD and treatment (*p*= 0.0037). Under OGD conditions there were greater levels of cell death when the media control was compared with 10mM 4-PBA (p=0.0001). After 24 h of recovery from OGD or normoxia with 4-PBA treatment (Fig. 6D), there was a significant effect of OGD (*p*<0.0001) and the effect of treatment approached, but did not reach significance (*p*=0.0570). There was no significant interaction between OGD and treatment (p=0.6852). Under OGD conditions there were greater levels of cell death when the media control was compared with 10mM 4-PBA (p=0.0395).

Inhibition and induction of autophagy during OGD increased cell death.

Hamartin mediated its neuroprotective effects through productive autophagy (2) and so we tested the effects of an autophagy inducer and an autophagy inhibitor directly on neuronal death during OGD. To inhibit autophagy, we used 3MA, a selective inhibitor of the class III PI3K which has been shown to inhibit beclin-1-dependent autophagy in several disease models (16). At 2 h of OGD or normoxia with 3MA treatment (Fig. 7A), there was a significant effect of OGD (*p*<0.0001) and treatment (*p*=0.004) on cell death. There was a significant interaction between OGD and treatment (*p*=0.0392). Under OGD conditions there were greater levels of cell death following treatment with 10µM 3MA compared to DMSO (*p*=0.0003). After 24 h of recovery from OGD or normoxia with 3MA treatment (Fig. 7B), there was a significant effect of OGD (*p*<0.0001) and treatment (*p*<0.0001). There was a significant interaction between OGD and treatment (*p*=0.0424). There were greater levels of cell death when the DMSO control was compared with 10µM 3MA in normoxia (*p*=0.0347) and OGD (*p*=0.0001).

To induce autophagy, we used 10-NCP, an Akt inhibitor, which has been shown to upregulate autophagy in a primary neuronal model of Huntington's disease (17). At 2 h of OGD or normoxia with 10-NCP treatment (Fig. 7C), there was a significant effect of OGD (*p*=0.0290), there was however no significant effect of treatment (*p*=0.3540) (two-way ANOVA) on cell death. There was also no significant interaction between OGD and treatment (*p*= 0.1491). After 24 h of recovery from OGD or normoxia with 10-NCP treatment (Fig. 7D), there was no significant effect of OGD (*p*=0.0767). Treatment was significant (*p*<0.0001). There was a significant interaction between OGD and treatment (*p*=0.0002). Under normoxic conditions there were greater levels of cell death when the media control was compared with 10μM 10-NCP (*p*<0.0001) and under OGD conditions when the media control was compared with 1μM 10-NCP (*p*=0.0201).

Discussion

This study has explored how global ischemia alters the ER stress response spatially and temporally in the hippocampus, whether pharmacological modulation of ER stress and autophagy could influence neuronal survival and explain, in part, the mechanism for hamartin's endogenous neuroprotective effect. A downregulation of hamartin expression 3 h following global forebrain ischemia in the vulnerable CA1 region of the hippocampus replicates previous findings showing that hamartin expression is associated with neuronal survival (2). Changes in the expression of ER stress proteins at 3 and 12 h post-ischemia in vulnerable and resistant areas of the hippocampus might reveal a viable pharmacological target downstream of hamartin. However, direct pharmacological modulation of ER stress in primary neurons resulted in neurotoxicity rather than neuroprotection. Similarly, inhibition of autophagy was neurotoxic and induction of autophagy alone failed to demonstrate neuroprotection.

In our model, there was a differential ER stress response to 10 min of global ischemia. Following 3 h of reperfusion, there was a significant decrease in ER stress proteins phospho-eIF2α and ATF4 in the tolerant CA3 region of the hippocampus. This suggests that a decrease in ER stress at 3 h is associated with neuronal survival, given that CA3 neurons survive the ischemic insult (2) out to 7 days. This is in keeping with current literature, where in a two vessel occlusion/hypotension model of global ischemia, the ER stress response to ischemia was found to be stronger in CA1 than CA3 (8). In addition, neurons lacking the TSC1/TSC2 complex have increased vulnerability to ER stress-induced cell death via the activation of the mitochondrial death pathway (3). These results provide evidence that ER stress inhibition may be a viable therapeutic target to protect neurons following ischemic injury.

Corroborating previous studies, there was a significant increase in CA1 ER stress protein expression following 12 h of reperfusion, but ER stress activity was not present at 3 h of reperfusion. This delayed ER stress response could be associated with the neuronal death that eventually occurs in CA1 following global ischemia. This is in line with previous findings that ER stress markers phospho-eIF2α and PERK were increased in CA1 neurons following ischemia in a rodent model (7). ATF4 is known to be activated by severe ER stress and both ATF4 and ER stress play a role in apoptosis (7). In wild-type and human copper/zinc superoxide dismutase transgenic rats, following global ischemia, increased levels of ATF4 and CHOP were measured in CA1 neurons that would undergo apoptotic cell death (18). In the gerbil model of transient forebrain ischemia, ER stress has also been implicated in neuronal cell death demonstrated in the CA1 region of the hippocampus (19). The temporal association between decreased hamartin expression and increased ER stress levels in CA1 neurons suggests that the presence of hamartin may block the ER stress response, which alongside autophagy induction, could be mediating hamartin's endogenous protective effect.

In agreement with previous reports, the ER stress inducers, thapsigargin and tunicamycin resulted in increased cell death *in vitro* when added to cortical neurons during 2 h of normoxia or OGD. This supports the notion that ER stress is detrimental to neuronal cell survival per se as well as following ischemia. Mild ER stress has been shown to lead to autophagy (20, 21) which could be protective, but in our experiments low doses of thapsigargin or tunicamycin did not improve neuronal survival.

While it was expected that an ER stress inhibitor would afford neuroprotection, treatment with salubrinal dose dependently increased cell death following 2 h of normoxia and OGD. A previous study has shown detrimental effects of salubrinal by abolishing the protection by ER stress-induced autophagy in an *in vivo* focal rodent stroke model (5). However, other studies have shown that salubrinal decreased neuronal death in experimental rodent models of excitotoxicity, epilepsy and focal ischemia (22, 23). In our *in vitro* experiments, salubrinal exhibited neurotoxic effects, potentially by abolishing any protective effects of ER stress-induced autophagy. We then tested another ER stress inhibitor the chemical chaperone 4-PBA, and this also showed increased neuronal cell death following OGD, replicating the salubrinal data.

Induction of productive autophagy is another important pathway downstream of hamartin activation and has been associated with protection of CA3 neurons following ischemia (2). As expected inhibition of autophagy with 3MA caused neuronal death at high concentrations. However Induction of autophagy with 10-NCP also exacerbated neuronal death at high concentrations at 24 h following 2 h under normoxic and OGD conditions. There exists a complicated interplay between ER stress and autophagy. Indeed, there is emerging evidence that ER stress activation can lead to autophagy (20, 21), including in neurons (24). The protective effect of mild ER stress (preconditioning) is thought to be due to autophagy (25). The link between autophagy and ER stress is however not entirely clear, with evidence for involvement in all three of the stress sensor pathways. Autophagy can be activated by both PERK and ATF6 pathways (26, 27). A potential mechanism has been proposed whereby autophagy is enhanced via the ER stress-driven negative regulation of the Akt/TSC/mTOR pathway (28). To further complicate the relationship, autophagy may also modulate ER stress (29) and the ER may inhibit autophagy (30, 31). Moreover, ATF4 controls the expression of various genes involved in autophagy, apoptosis, amino acid metabolism, and antioxidant responses as reviewed by Hetz and Mollereau (32). It is clear that a greater mechanistic understanding of the particular points at which ER stress and productive autophagy switch from detrimental effects to beneficial effects or vice versa in the context of neuronal ischemia is required in order to harness any endogenous neuroprotection.

One limitation of our *in vitro* pharmacological experiments is the use of cortical neurons rather than hippocampal neurons. While our *in vivo* experiments focussed on the hippocampus and the divergence in neuronal susceptibility between the CA1 and CA3 neurons, it was not feasible to obtain the yields of hippocampal neurons required for our *in vitro* pharmacological investigation. Moreover, we have previously shown that the knockdown of hamartin in both cortical neurons and hippocampal neurons *in vitro* can lead to the same effect following exposure to OGD, i.e. hamartin knockdown exacerbates neuronal death (2). Therefore, there is a conservation of effect between our cortical and hippocampal neuronal preparations which justifies the use of cortical neurons for our pharmacological experiments.

In conclusion, the temporal association between hamartin expression and de(32)creased ER stress levels in CA3 neurons *in vivo* may contribute to the mechanism of hamartin's endogenous protective effect. *In vitro*, inducing ER stress had the expected result of increasing neuronal death but inhibition of ER stress also produced neurotoxicity, possibly via prevention of ER stress-induced autophagy. Inhibition of autophagy was neurotoxic and induction of autophagy alone failed to demonstrate a protective effect. Further studies are required to ascertain when ER stress becomes detrimental to neurons, and whether modulation of ER stress pharmacologically is a viable therapeutic strategy for cerebral ischemia.

Contributions

The experiments were conceived and designed by GH, KV, GCD, MP, BAS and AMB; experiments were carried out by GH, AAN, YC, DJB, BAA and BAS; experiments were analysed by GH, DJB and BAS; the paper was written by GH and BAS and edited by all authors.

Conflict of Interest

AMB is a senior medical science advisor and co-founder of Brainomix, a company that develops electronic ASPECTS (e-ASPECTS), an automated method to evaluate ASPECTS in stroke patients. MP is a co-founder and employee of Brainomix. All other authors declare no conflict of interest.

Funding Sources

GH was supported by the Oxford University Clinical Academic Graduate School. AAN was supported by a Radcliffe Department of Medicine Scholarship. YC, KV, DJB, BAA, GCD, BAS and AMB were supported by the Medical Research Council (UK). BAA was also supported by the Engineering and Physical Sciences Research Council.

References

1. Kirino T. Delayed neuronal death in the gerbil hippocampus following ischemia. Brain Res. 1982;239(1):57-69.
2. Papadakis M, Hadley G, Xilouri M, Hoyte LC, Nagel S, McMenamin MM, et al. Tsc1 (hamartin) confers neuroprotection against ischemia by inducing autophagy. Nat Med. 2013;19(3):351-7.

3. Di Nardo A, Kramvis I, Cho N, Sadowski A, Meikle L, Kwiatkowski DJ, et al. Tuberous sclerosis complex activity is required to control neuronal stress responses in an mTOR-dependent manner. J Neurosci. 2009;29(18):5926-37.
4. Cooper GM. The Cell: A Molecular Approach. 2nd ed: Sinauer Associates; 2000.
5. Gao B, Zhang XY, Han R, Zhang TT, Chen C, Qin ZH, et al. The endoplasmic reticulum stress inhibitor salubrinal inhibits the activation of autophagy and neuroprotection induced by brain ischemic preconditioning. Acta Pharmacol Sin. 2013;34(5):657-66.
6. Kumar R, Krause GS, Yoshida H, Mori K, DeGracia DJ. Dysfunction of the unfolded protein response during global brain ischemia and reperfusion. J Cereb Blood Flow Metab. 2003;23(4):462-71.
7. Hayashi T, Saito A, Okuno S, Ferrand-Drake M, Dodd RL, Nishi T, et al. Oxidative damage to the endoplasmic reticulum is implicated in ischemic neuronal cell death. J Cereb Blood Flow Metab. 2003;23(10):1117-28.
8. Roberts GG, Di Loreto MJ, Marshall M, Wang J, DeGracia DJ. Hippocampal cellular stress responses after global brain ischemia and reperfusion. Antioxid Redox Signal. 2007;9(12):2265-75.
9. Friedman DB, Lilley KS. Quantitative proteomics for two-dimensional gels using difference gel electrophoresis (DIGE) technology. In: Walker JM, editor. Protein Protocols. 3rd ed: Humana Press; 2009.
10. Vogiatzi T, Xilouri M, Vekrellis K, Stefanis L. Wild type alpha-synuclein is degraded by chaperone-mediated autophagy and macroautophagy in neuronal cells. J Biol Chem. 2008;283(35):23542-56.
11. Nguyen HN, Wang C, Perry DC. Depletion of intracellular calcium stores is toxic to SH-SY5Y neuronal cells. Brain Res. 2002;924(2):159-66.
12. Gascon S, Garcia-Gallo M, Renart J, Diaz-Guerra M. Endoplasmic reticulum-associated degradation of the NR1 but not the NR2 subunits of the N-methyl-D-aspartate receptor induced by inhibition of the N-glycosylation in cortical neurons. J Neurosci Res. 2007;85(8):1713-23.
13. Boyce M, Bryant KF, Jousse C, Long K, Harding HP, Scheuner D, et al. A selective inhibitor of eIF2alpha dephosphorylation protects cells from ER stress. Science. 2005;307(5711):935-9.
14. Ozcan U, Yilmaz E, Ozcan L, Furuhashi M, Vaillancourt E, Smith RO, et al. Chemical chaperones reduce ER stress and restore glucose homeostasis in a mouse model of type 2 diabetes. Science. 2006;313(5790):1137-40.
15. Ozcan U, Ozcan L, Yilmaz E, Duvel K, Sahin M, Manning BD, et al. Loss of the tuberous sclerosis complex tumor suppressors triggers the unfolded protein response to regulate insulin signaling and apoptosis. Mol Cell. 2008;29(5):541-51.
16. Kihara A, Kabeya Y, Ohsumi Y, Yoshimori T. Beclin-phosphatidylinositol 3-kinase complex functions at the trans-Golgi network. EMBO Rep. 2001;2(4):330-5.
17. Tsvetkov AS, Miller J, Arrasate M, Wong JS, Pleiss MA, Finkbeiner S. A small-molecule scaffold induces autophagy in primary neurons and protects against toxicity in a Huntington disease model. Proc Natl Acad Sci U S A. 2010;107(39):16982-7.
18. Hayashi T, Saito A, Okuno S, Ferrand-Drake M, Dodd RL, Chan PH. Damage to the endoplasmic reticulum and activation of apoptotic machinery by oxidative stress in ischemic neurons. J Cereb Blood Flow Metab. 2005;25(1):41-53.
19. Oida Y, Izuta H, Oyagi A, Shimazawa M, Kudo T, Imaizumi K, et al. Induction of BiP, an ER-resident protein, prevents the neuronal death induced by transient forebrain ischemia in gerbil. Brain Res. 2008;1208:217-24.
20. Sakaki K, Kaufman RJ. Regulation of ER stress-induced macroautophagy by protein kinase C. Autophagy. 2008;4(6):841-3.
21. Yorimitsu T, Nair U, Yang Z, Klionsky DJ. Endoplasmic reticulum stress triggers autophagy. J Biol Chem. 2006;281(40):30299-304.
22. Nakka VP, Gusain A, Raghubir R. Endoplasmic reticulum stress plays critical role in brain damage after cerebral ischemia/reperfusion in rats. Neurotox Res. 2010;17(2):189-202.

23. Sokka AL, Putkonen N, Mudo G, Pryazhnikov E, Reijonen S, Khiroug L, et al. Endoplasmic reticulum stress inhibition protects against excitotoxic neuronal injury in the rat brain. J Neurosci. 2007;27(4):901-8.
24. Sheng R, Liu XQ, Zhang LS, Gao B, Han R, Wu YQ, et al. Autophagy regulates endoplasmic reticulum stress in ischemic preconditioning. Autophagy. 2012;8(3):310-25.
25. Bernales S, McDonald KL, Walter P. Autophagy counterbalances endoplasmic reticulum expansion during the unfolded protein response. PLoS Biol. 2006;4(12):e423.
26. Ogata M, Hino S, Saito A, Morikawa K, Kondo S, Kanemoto S, et al. Autophagy is activated for cell survival after endoplasmic reticulum stress. Mol Cell Biol. 2006;26(24):9220-31.
27. Rouschop KM, van den Beucken T, Dubois L, Niessen H, Bussink J, Savelkouls K, et al. The unfolded protein response protects human tumor cells during hypoxia through regulation of the autophagy genes MAP1LC3B and ATG5. J Clin Invest. 2010;120(1):127-41.
28. Qin L, Wang Z, Tao L, Wang Y. ER stress negatively regulates AKT/TSC/mTOR pathway to enhance autophagy. Autophagy. 2010;6(2):239-47.
29. Carloni S, Albertini MC, Galluzzi L, Buonocore G, Proietti F, Balduini W. Increased autophagy reduces endoplasmic reticulum stress after neonatal hypoxia-ischemia: role of protein synthesis and autophagic pathways. Exp Neurol. 2014;255:103-12.
30. Bassik MC, Scorrano L, Oakes SA, Pozzan T, Korsmeyer SJ. Phosphorylation of BCL-2 regulates ER Ca2+ homeostasis and apoptosis. EMBO J. 2004;23(5):1207-16.
31. Pattingre S, Tassa A, Qu X, Garuti R, Liang XH, Mizushima N, et al. Bcl-2 antiapoptotic proteins inhibit Beclin 1-dependent autophagy. Cell. 2005;122(6):927-39.
32. Hetz C, Mollereau B. Disturbance of endoplasmic reticulum proteostasis in neurodegenerative diseases. Nat Rev Neurosci. 2014;15(4):233-49.

Figure Legends:

Figure 1 Experimental protocols. A) Male Wistar rats underwent pre-four vessel occlusion (4-VO) surgery on day 1 which included placing loose sutures around the common carotid arteries, cauterizing the vertebral arteries, and inserting a suture through the neck to enable control of collateral circulation. On day 2, 4-VO took place where both common carotid arteries were clamped and the neck suture tightened to completely restrict blood flow to the forebrain. Ischemia lasted for 10 min before the carotid clamps were removed and the neck suture loosened. Rats were recovered for 3 h or 12 h before being killed and immunoblotted for hamartin and ER stress proteins. **B)** Primary cortical neurons were isolated from E18 Wistar rat embryos and cultured for 7 days prior to experiments. On the day of the experiment, neurons were exposed to oxygen and glucose deprivation (OGD) or normoxia in the presence of glucose as a control for 2 h. During this time, pharmacological agents or vehicle controls were added to the media. After 2 h, media was removed for later cell death analysis using the lactate dehydrogenase (LDH) assay. Recovery media (normoxia + glucose) were then added to the cells and incubated for 24 h at which time media was removed for LDH assessment.

Figure 2 Hamartin expression in CA1 of hippocampus at 3 h following 10 min of global cerebral ischemia Upper panel (A) shows the western blots and loading correction with Sypro used to produce the graph (B) of hamartin immunoreactivity. (B) CA1 sham (n=7) and CA1 ischemia (n=7). $^{**}p<0.01$ Molecular weight: 160 kDa.

Figure 3 Time course for expression of ER stress protein, ATF4 which is reduced in the resistant hippocampal CA3 region at 3 h and increased in the vulnerable CA1 region at 12 h following 10 min of global cerebral ischemia. At 3 h: A) ATF4 (CREB 2) expression was not changed between 4-VO and sham animals in the CA1 region. B) There were significantly lower ATF4 (CREB 2) levels in CA3 at 3 h following ischemia compared to sham. At 12 h: C) ATF4 (CREB 2) expression was increased following 4-VO compared to sham animals in the CA1 region. D) There was no change in ATF4 (CREB 2) expression between groups in the CA3 region. In all sub-figures, upper panels show the Western blots and loading correction with Sypro® used to produce the lower panels quantifying ATF4 immunoreactivity. $^{*}p<0.05$. In 12 h experiments two animals were excluded as they did not meet criteria for ischemia.

Figure 4 ER stress protein, Phospho-eIF2α expression was reduced in the resistant hippocampal CA3 region 3 h and increased at 12 h following 10 min of global cerebral ischemia. A) There were significantly lower phospho-eIF2α levels in CA3 at 3 h following ischemia compared to sham. B) Phospho-eIF2α expression was augmented following 4-VO compared to sham animals in the CA1 region. In all sub-figures, upper panels show the Western blots and loading correction with Sypro® used to produce the lower panels quantifying phospho-eIF2α immunoreactivity. $^{*}p<0.05$. In 12 h experiments two animals were excluded as they did not meet criteria for ischemia.

Figure 5 ER stress induction during OGD increased cell death. High dose (10μM) thapsigargin administration during 2 h OGD increased cell death at 2h (A) and 24 h recovery (B). 10μM thapsigargin also increased cell death following 2h normoxia and 24h recovery (B). DMSO (n=9), 0.01μM thapsigargin (n=6), 0.1μM thapsigargin (n=6), 1μM thapsigargin (n=6) or 10μM thapsigargin (n=3). During 2h OGD, high dose (1μM) tunicamycin increased cell death (C) but this increase did not remain following 24 h recovery (D). DMSO (n=3), 0.01μM tunicamycin (n=3), 0.1μM tunicamycin (n=3) or 1μM tunicamycin (n=3). $^{**}p<0.01$, $^{****}p<0.0001$. Cell death was quantified by LDH assay.

Figure 6 ER stress inhibition during OGD increased cell death. A) Salubrinal had no effect on cortical neuronal death at 2h OGD. B) High dose (200µM and 500µM) salubrinal increased cell death significantly following 2h OGD and 24h recovery. DMSO (n=6), 25µM salubrinal (n=9), 50µM salubrinal (n=9), 100µM salubrinal (n=9), 200µM salubrinal (n=3), 500µM salubrinal (n=3). High dose 4-PBA (10mM) increased cortical neuronal death at 2h C) and at 2h and 24 h D) recovery in OGD conditions. Media (n=12), 10µM 4-PBA (n=6), 100µM 4-PBA (n=12), 1mM 4-PBA (n=12), 10mM 4-PBA (n=6). Cell death was quantified by LDH assay.*p<0.05, **p<0.01, ****p<0.0001.

Figure 7 Inhibition and induction of autophagy during OGD increased cell death. A) 10µM 3-MA (autophagy inhibitor) increased cortical neuronal death at 2h OGD. B) 10µM 3-MA increased cortical neuronal death at 24h recovery in normoxia and OGD conditions. All n=3-6. C) 10-NCP (autophagy inducer) had no effect on cortical neuronal death at 2h OGD. D) 10µM 10-NCP increased cortical neuron death at 24h recovery following 2h normoxia while 1µM 10-NCP increased cortical neuron death at 24h recovery following 2h OGD. All n=6. Cell death was quantified by LDH assay.*p<0.05, ***p<0.001, ****p<0.0001.

Figure 1

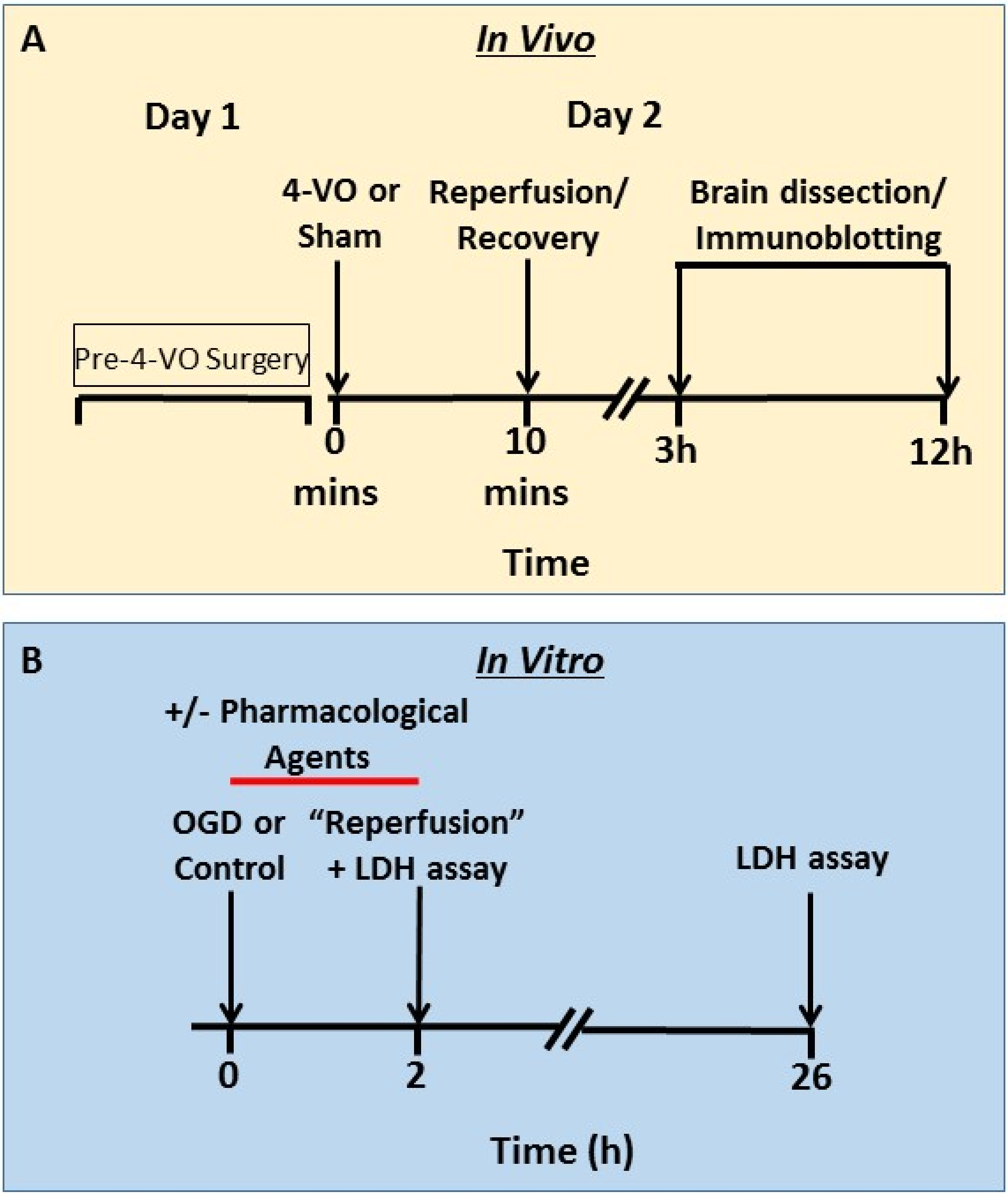
A
In Vivo
Day 1
Day 2
4-VO or Sham
Reperfusion/ Recovery
Brain dissection/ Immunoblotting
Pre-4-VO Surgery
0 mins
10 mins
3h
12h
Time
B
In Vitro
+/- Pharmacological Agents
OGD or Control
"Reperfusion" + LDH assay
LDH assay
0
2
26
Time (h)

Figure 2

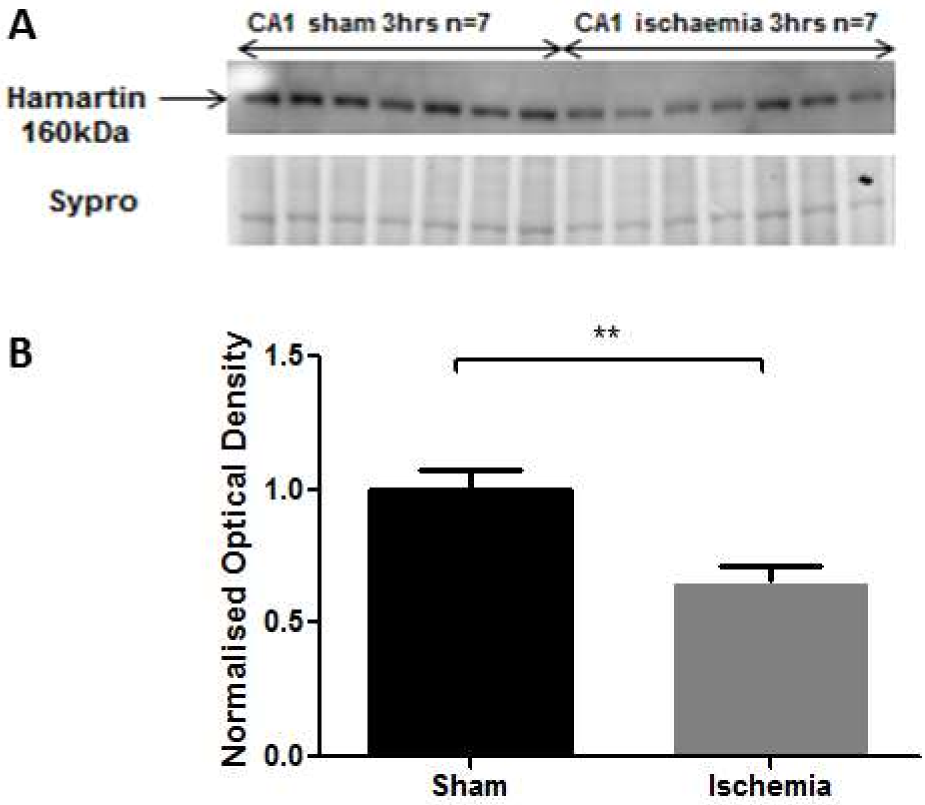
A
CA1 sham 3hrs n=7
CA1 ischaemia 3hrs n=7
Hamartin
160kDa
Sypro
B
Normalised Optical Density
1.5
1.0
0.5
0.0
**
Sham
Ischemia

Figure 3

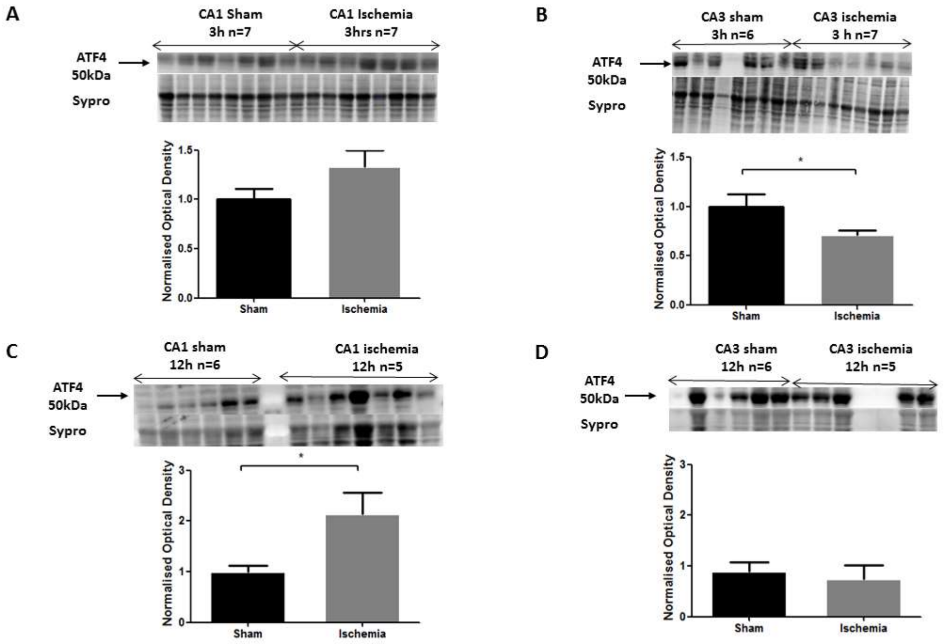
A
CA1 Sham 3h n=7
CA1 Ischemia 3hrs n=7
ATF4 50kDa
Sypro
Normalised Optical Density
1.5
1.0
0.5
0.0
Sham
Ischemia
B
CA3 sham 3h n=6
CA3 ischemia 3 h n=7
ATF4 50kDa
Sypro
*
Normalised Optical Density
1.5
1.0
0.5
0.0
Sham
Ischemia
C
CA1 sham 12h n=6
CA1 ischemia 12h n=5
ATF4 50kDa
Sypro
*
Normalised Optical Density
3
2
1
0
Sham
Ischemia
D
CA3 sham 12h n=6
CA3 ischemia 12h n=5
ATF4 50kDa
Sypro
Normalised Optical Density
3
2
1
0
Sham
Ischemia

Figure 4

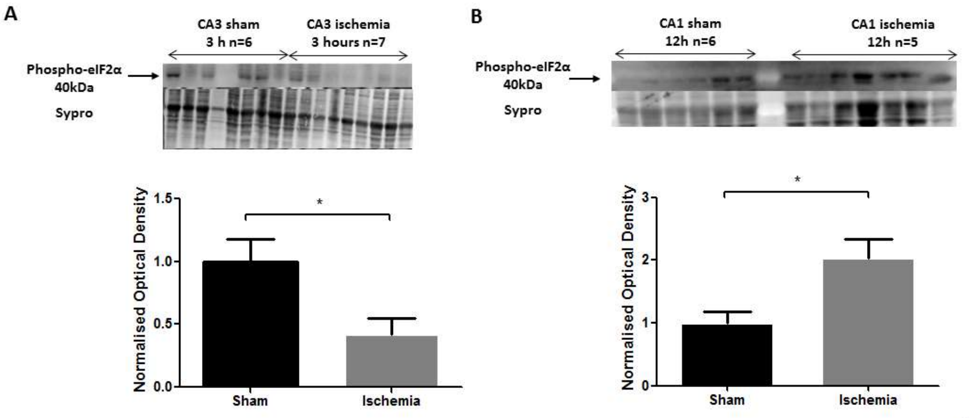
A
CA3 sham
3 h n=6
CA3 ischemia
3 hours n=7
Phospho-eIF2α
40kDa
Sypro
Normalised Optical Density
1.5
1.0
0.5
0.0
*
Sham
Ischemia
B
CA1 sham
12h n=6
CA1 ischemia
12h n=5
Phospho-eIF2α
40kDa
Sypro
Normalised Optical Density
3
2
1
0
*
Sham
Ischemia

Figure 5

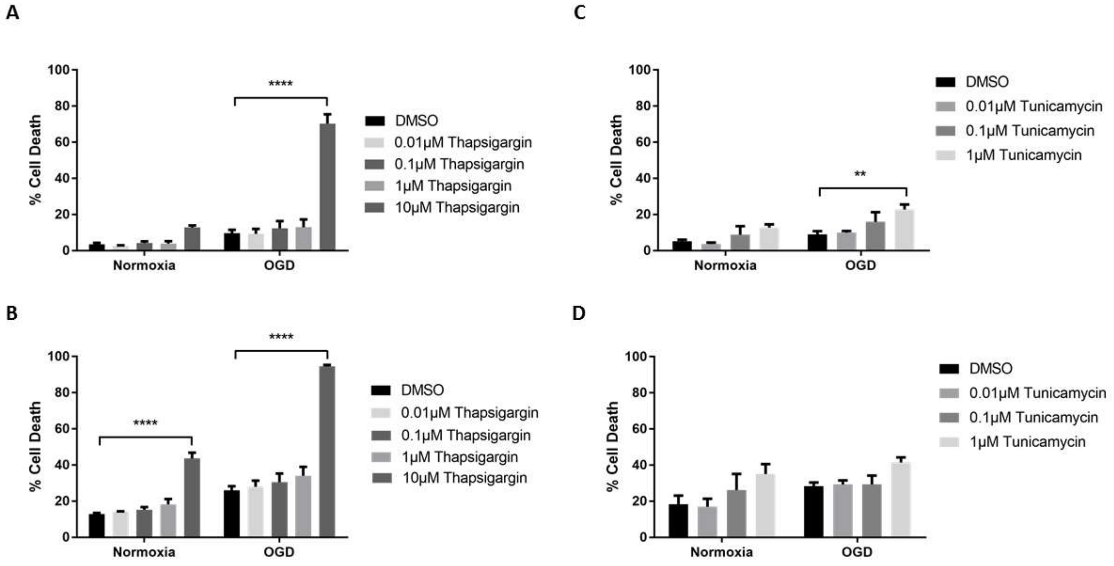
A
100
80
60
40
20
0
% Cell Death
Normoxia
OGD
****
DMSO
0.01μM Thapsigargin
0.1μM Thapsigargin
1μM Thapsigargin
10μM Thapsigargin
B
100
80
60
40
20
0
% Cell Death
Normoxia
OGD
****
****
DMSO
0.01μM Thapsigargin
0.1μM Thapsigargin
1μM Thapsigargin
10μM Thapsigargin
C
100
80
60
40
20
0
% Cell Death
Normoxia
OGD
**
DMSO
0.01μM Tunicamycin
0.1μM Tunicamycin
1μM Tunicamycin
D
100
80
60
40
20
0
% Cell Death
Normoxia
OGD
DMSO
0.01μM Tunicamycin
0.1μM Tunicamycin
1μM Tunicamycin

Figure 6

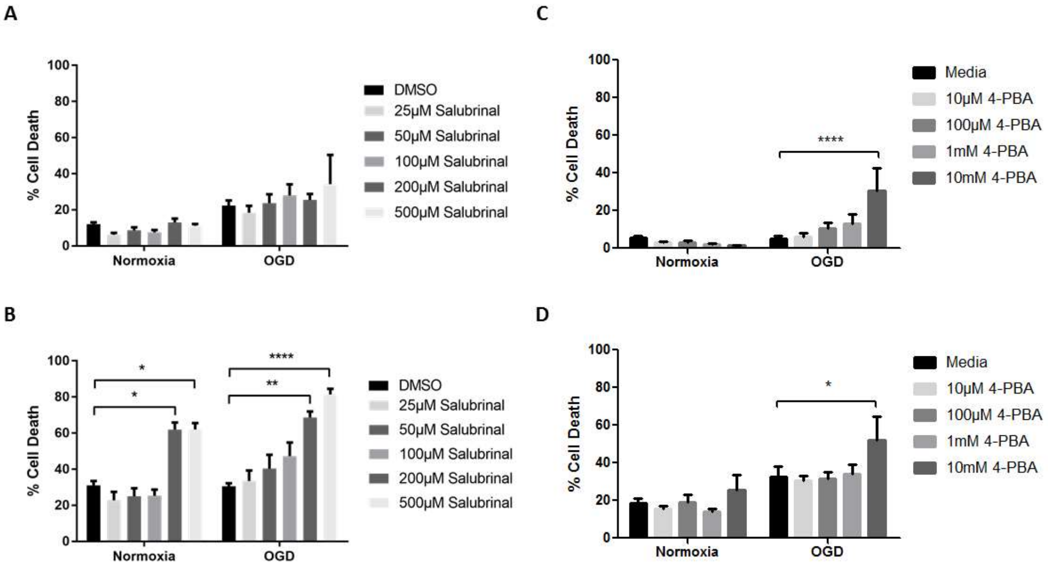
A
% Cell Death
100
80
60
40
20
0
Normoxia
OGD
DMSO
25μM Salubrinal
50μM Salubrinal
100μM Salubrinal
200μM Salubrinal
500μM Salubrinal
B
% Cell Death
100
80
60
40
20
0
*
*
****
**
Normoxia
OGD
DMSO
25μM Salubrinal
50μM Salubrinal
100μM Salubrinal
200μM Salubrinal
500μM Salubrinal
C
% Cell Death
100
80
60
40
20
0
****
Normoxia
OGD
Media
10μM 4-PBA
100μM 4-PBA
1mM 4-PBA
10mM 4-PBA
D
% Cell Death
100
80
60
40
20
0
*
Normoxia
OGD
Media
10μM 4-PBA
100μM 4-PBA
1mM 4-PBA
10mM 4-PBA

Figure 7

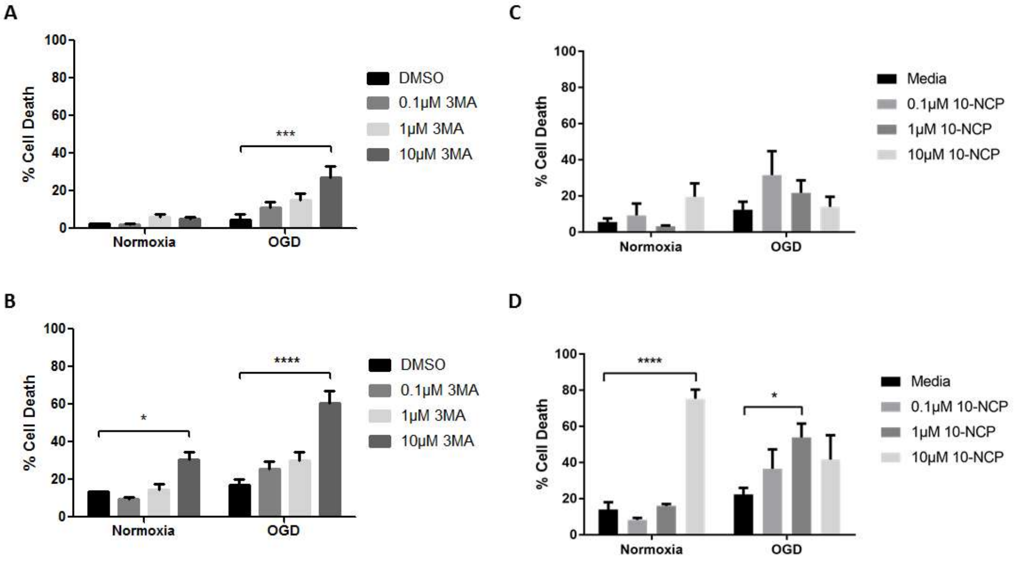
A
% Cell Death
100
80
60
40
20
0
Normoxia
OGD
***
DMSO
0.1µM 3MA
1µM 3MA
10µM 3MA
B
% Cell Death
100
80
60
40
20
0
Normoxia
OGD
*
****
DMSO
0.1µM 3MA
1µM 3MA
10µM 3MA
C
% Cell Death
100
80
60
40
20
0
Normoxia
OGD
Media
0.1µM 10-NCP
1µM 10-NCP
10µM 10-NCP
D
% Cell Death
100
80
60
40
20
0
Normoxia
OGD
****
*
Media
0.1µM 10-NCP
1µM 10-NCP
10µM 10-NCP